

# Cumulus Cell Transcripts Transit to the Bovine Oocyte in Preparation for Maturation<sup>1</sup>

Angus D. Macaulay,<sup>3</sup> Isabelle Gilbert,<sup>3</sup> Sara Scantland,<sup>3</sup> Eric Fournier,<sup>3</sup> Fazl Ashkar,<sup>4</sup> Alexandre Bastien,<sup>3</sup> Habib A. Shojaei Saadi,<sup>3</sup> Dominic Gagné,<sup>3</sup> Marc-André Sirard,<sup>3</sup> Édouard W. Khandjian,<sup>5</sup> François J. Richard,<sup>3</sup> Poul Hyttel,<sup>6</sup> and Claude Robert<sup>2,3</sup>

<sup>3</sup>Département des sciences animales, Centre de recherche en biologie de la reproduction, Institut sur la nutrition et les aliments fonctionnels, Université Laval, Québec, Québec, Canada

<sup>4</sup>Department of Biomedical Sciences, Reproductive Biology Lab, University of Guelph, Guelph, Ontario, Canada

<sup>5</sup>Département de Psychiatrie et Neurosciences, Institut universitaire en santé mentale de Québec, Université Laval, Québec City, Québec, Canada

<sup>6</sup>Department of Veterinary Clinical and Animal Sciences, Faculty of Health and Medical Sciences, University of Copenhagen, Copenhagen, Denmark

## ABSTRACT

So far, the characteristics of a good quality egg have been elusive, similar to the nature of the physiological, cellular, and molecular cues leading to its production both in vivo and in vitro. Current understanding highlights a strong and complex interdependence between the follicular cells and the gamete. Secreted factors induce cellular responses in the follicular cells, and direct exchange of small molecules from the cumulus cells to the oocyte through gap junctions controls meiotic arrest. Studying the interconnection between the cumulus cells and the oocyte, we previously demonstrated that the somatic cells also contribute transcripts to the gamete. Here, we show that these transcripts can be visualized moving down the transzonal projections (TZPs) to the oocyte, and that a time course analysis revealed progressive RNA accumulation in the TZPs, indicating that RNA transfer occurs before the initiation of meiosis resumption under a timetable fitting with the acquisition of developmental competence. A comparison of the identity of the nascent transcripts trafficking in the TZPs, with those in the oocyte increasing in abundance during maturation, and that are present on the oocyte's polyribosomes, revealed transcripts common to all three fractions, suggesting the use of transferred transcripts for translation. Furthermore, the removal of potential RNA trafficking by stripping the cumulus cells caused a significant reduction in maturation rates, indicating the need for the cumulus cell RNA transfer to the oocyte. These results offer a new perspective to the determinants of oocyte quality and female fertility, as well as provide insight that may eventually be used to improve in vitro maturation conditions.

*cumulus cells, maturation, oocyte, RNA transfer, transzonal projection*

<sup>1</sup>Funding of this project was provided by the Fonds québécois de la recherche sur la nature et les technologies (grants 2013-PR-138708 and 2015-PR-182922) and the Canadian Institute of Health Research—Institute of Human Development, Child and Youth Health (CAP-120358).

<sup>2</sup>Correspondence: E-mail: [claudio.robert@fsaa.ulaval.ca](mailto:claudio.robert@fsaa.ulaval.ca)

Received: 12 December 2014.  
First decision: 1 February 2015.  
Accepted: 13 November 2015.

© 2016 by the Society for the Study of Reproduction, Inc. This article is available under a Creative Commons License 4.0 (Attribution-Non-Commercial), as described at <http://creativecommons.org/licenses/by/4.0>.  
eISSN: 1529-7268 <http://www.biolreprod.org>  
ISSN: 0006-3363

## INTRODUCTION

It is known that mammalian oocytes spontaneously resume meiosis once extracted from their follicular environment and placed in in vitro culture [1]. Despite 35 y of in vitro fertilization research we still have a limited understanding of the involved processes. In all mammalian species, in vitro maturation (IVM) of fully grown oocytes from small follicles translates into lower embryonic developmental rates compared with in vivo-matured counterparts [2, 3]. Human oocytes matured in vitro typically do so at rates between 50% and 70%, and often less than half of those matured oocytes reach blastocyst stage [2, 4], although recent work has shown that this is improving in follicle-stimulating hormone (FSH)-stimulated women, whose cohorts included small follicles [5]. Cattle represent a good model, being a mono-ovular species, typically having about 80% of oocytes reaching metaphase two (MII) and comparable to human ( $\approx 35\%$ ) blastocyst development after IVM [6, 7]. This diminished performance of in vitro versus in vivo conditions on oocyte maturation and development has been imputed to a lack of understanding oocyte requirements [8]. These suboptimal success rates indicate that events within the follicle are not recapitulated by in vitro conditions, leaving the oocyte less prepared for embryogenesis [3]. It has been shown that oocyte quality prior to maturation is the most influential factor in the developmental potential required to reach blastocyst stage and that in vivo conditions are heavily influenced by the hormonal regime given for ovarian stimulation [3, 9–11]. Manipulations of the conditions both in vivo through control over hormonal regimen [9, 10] as well as in vitro by monitoring the time of oocyte collection following slaughter [12], or by controlling meiosis resumption have been described to increase developmental competence [7]. From this arose the concept of oocyte prematuration, where IVM conditions can be manipulated to prevent spontaneous meiotic resumption, with the objective of improving the oocyte's developmental competence [7, 13].

The current model of mammalian oogenesis is known to involve bidirectional communication between the surrounding cumulus cells and the oocyte, orchestrating growth and maturation of both the gamete and follicular compartments. The existing model for this bilateral communication involves paracrine signaling and small molecule (<1 kDa) exchange via gap junctions [14–16]. Direct transfer of small molecules is permitted through the cumulus cell projections that penetrate the zona pellucida and make contact with the oolemma (transzonal projections [TZPs]). At the edge of the projection,

intermediate junctions (zonula adherens-like junctions) keep the cytoplasmic membranes of both cells in close contact, and gap junctions allow the exchange of the small molecules, namely cAMP and cGMP [17, 18]. Although these large macro channels are present, uptake of large molecules by the oocyte is not believed to occur [19]. We have recently shown that, contrarily to what has been observed previously, exchange of large cargo—including de novo-synthesized long RNA, defined as longer than 200 bp in length—molecules can occur between the cumulus cells and the oocyte through the TZPs [20].

The aim of this study is to determine, based on our previous observations, the potential roles played by these transferred RNAs in oocyte maturation. We hypothesized that the cumulus cells transfer mRNAs benefitting oocyte maturation in an orchestrated fashion. We further explore our recently identified mechanism by which cumulus cells contribute to oocyte development and maturation by providing large RNA molecules. A better knowledge of this transfer could be pivotal to the definition of egg quality and its intrinsic potential to undertake and sustain early embryonic development.

## MATERIALS AND METHODS

All chemicals were purchased from Sigma Chemical Co. unless otherwise indicated.

### *Oocyte Collection and Maturation*

All animals were slaughtered in accordance with the Canadian Food Inspection Agency standards. Their regulations were followed strictly at the local abattoir that provided the ovaries. No animals were handled on university premises. Bovine oocytes were collected from 2- to 6-mm follicles from abattoir ovaries. Good quality oocytes displaying homogenous cytoplasm, a complete cumulus cloud with no signs of atresia, and a fully grown size greater than 120  $\mu\text{m}$  were selected. Cumulus-oocyte complexes (COCs) were typically matured in standard maturation medium as previously described [10]. If oocytes were denuded, it was done so by gentle mechanical pipetting for 1 min in a four-well dish, followed by further media washing prior to maturation. Maturation medium was composed of TCM199 (Gibco 11150059; Life Technologies), 10% fetal bovine serum, 0.2 mM pyruvate, 50  $\mu\text{g}/\text{ml}$  gentamicin, 5  $\mu\text{g}/\text{ml}$  FSH (Serono), and 1  $\mu\text{g}/\text{ml}$   $\text{E}_2$ . Oocytes were matured in groups of 50 in 500  $\mu\text{l}$  of media at 38.5 °C with 5%  $\text{CO}_2$  in air with maximal humidity. However, in the timing of the TZP RNA loading experiment, oocytes were collected from ovaries at the abattoir at specific time points (0, 2, 4, and 6 h) following slaughter, and maturation was conducted in a proprietary maturation medium with 10 oocytes per 500  $\mu\text{l}$  in a 0.6-ml Eppendorf tube (Boviteq Inc.) suitable for atmospheric gas in a portable incubator (Micro Q Technologies).

### *Transmission Electron Microscopy and Autoradiography*

Collected COCs were placed into equilibrated maturation media under oil for maturation. Oocytes were exposed to [ $^3\text{H}$ ]-uridine during the first 3 h of maturation. Transmission electron microscopy was carried out as described previously [21]. Briefly, exposed oocytes were transferred into media with a concentration of 200  $\mu\text{Ci}/\text{ml}$  [ $^3\text{H}$ ]-uridine (Perkin-Elmer). All COCs were washed twice in PBS supplemented with 10% fetal calf serum for 15 min at 4°C. Oocytes were fixed in freshly prepared 3% glutaraldehyde (Electron Microscope Solutions) in 1 $\times$  PBS for 1 h at 4°C. Prior to embedding, the oocytes were stored in 1 $\times$  PBS. Then, samples were postfixed in 1% osmium tetroxide (Alfa Aesar) in Na-phosphate buffer (pH 7.4) for 60 min, and rapidly dehydrated in increasing ethanol concentrations and embedded in epoxy resin (TAAB 812 Epon; TAAB). Ultrathin sections were cut using an ultramicrotome, and sample sections were stained with uranyl acetate (UltraStain; Laurylab) and with Reynolds lead citrate (Ampliqon). Autoradiographic exposure was performed using L4 emulsion (Ilford Nuclear Research Emulsion) and D19 developer (Kodak). Grids were viewed with transmission electron microscopy (JEM-1200 EX; Jeol).

### *Image Analysis: Quantification of Pixel Intensity and Density*

Pixel counting and density measurements were made using ImageJ (version 2.0.0). The threshold function allowed for the identification of pixels resulting from the autoradiographic signal. In the ultrathin sections, pixel density was measured as a percentage above threshold in defined areas: the zona pellucida, TZPs, cumulus cells, ooplasm, and intercellular regions like the perivitellin space, as well as the spaces between cumulus cells, to provide an assessment of the level of intercellular background. A total of 12 COCs, including some partially denuded ones, were processed and evaluated. Treated and exposed grids were also produced without cellular sections to provide another measure of background (nine images from six different control grids). The signal in the ultrathin sections was evaluated by region; that is, pinwheel segments were created on the image designated within the ooplasm. A similar analysis of RNA by fluorescent labeling of nascent RNA was done using the 5-ethyl uridine Click-iT Kit (Life Technologies). Each maximum-intensity projection composite image was taken at the equator of the oocyte— $n = 9$  cumulus-enclosed oocytes,  $n = 11$  partially denuded oocytes, and  $n = 12$  denuded oocytes—and contained 11 sections spanning 10  $\mu\text{m}$  of depth. Rhodamine phalloidin counterstaining of the actin cytoskeleton was also performed and evaluated to produce an RNA:actin ratio to normalize for the areas of the oocyte obstructed by the cumulus cells and cytoplasm during confocal acquisition. A further background correction was made based on extracellular regions and was subtracted from the ratio values to provide an average corrected intensity. ImageJ and MatLab software was used for image analysis. The same pinwheel overlay was produced to fit the oocyte's shape and to divide the oocyte into planes for regional analysis of the ooplasm in denuded, partially denuded, and cumulus-enclosed oocytes. Images of RNase-treated COCs incubated with the 5-ethyl uridine were also made to confirm the signal was from detected RNA.

### *Live Cell Imaging of RNA*

Immediately following aspiration, the RNA within the oocytes was stained using Syto RNA Select (1:1000 dilution; Life Technologies) for 30 min and washed. For live cell imaging, oocytes were placed in maturation media in an interchangeable coverslip dish (Bioprotech), including a custom-made chamber containing 60 wells of 280- $\mu\text{m}$  diameter each. The dish was laid into the microscope custom-made chamber at 37°C in a humidified atmosphere at 37°C. Confocal images of a single plane were taken using a Zeiss LSM 740 confocal live cell system (Karl Zeiss) at intervals ranging between 1.5 and 8 sec.

### *Isolation of Oocyte Polyribosomes and Microarray Transcript Evaluation*

Polyribosomes were isolated using pools of 75 germinal vesicle (GV) and MII oocytes using a previously described procedure [22]. Three biological replicates were performed for each maturation state. Briefly, the oocyte samples were spiked with *Drosophila* polyribosomes that had been chemically cross-linked and neutralized. These exogenous polyribosomes acted as a carrier and allowed for polyribosome detection during fractionation on a sucrose gradient. Proven polyribosomal fractions were isolated, and the bulk of *Drosophila* RNA was eliminated during total RNA extraction. Polyribosomal transcripts were identified by microarray hybridization (EmbryoGENE bovine 44 k oligo array, printed by Agilent) as described previously [23]. Microarray raw data are available at Gene Expression Omnibus (GEO) under accession number GSE56603. Because all samples were spiked with the same batch of carrier polyribosomes, *Drosophila* transcripts for which oligos were present on the microarrays served as internal standards for data normalization accounting for sample loss during the procedures, and also preserving the natural differences in polyribosomal RNA contents between both states of oocyte maturity.

### *RNA-seq Libraries Preparation and Sequencing*

Two RNA-seq analyses were conducted. In the first one, for total RNA transcriptome analysis, three pools, each containing 20 oocytes, were collected for each maturation stage (e.g., GV and MII). Total RNA extraction and DNase I treatment were performed using PicoPure columns (Life Technologies). The synthetic transcriptome ERCC (Life Technologies) was spiked in the extraction buffer that was distributed equally in all samples. Next, cDNA first- and second-strand synthesis was carried out using NuGen's Ovation kit. The cDNA was then amplified with NuGen's SPIA system. The final cDNA product was fragmented, ligated, and primed with bar-coded adaptors for RNA-seq using the Encore kit (NuGen). The exogenous RNA spike-in control mix was used for normalization to account for sample loss during sample processing

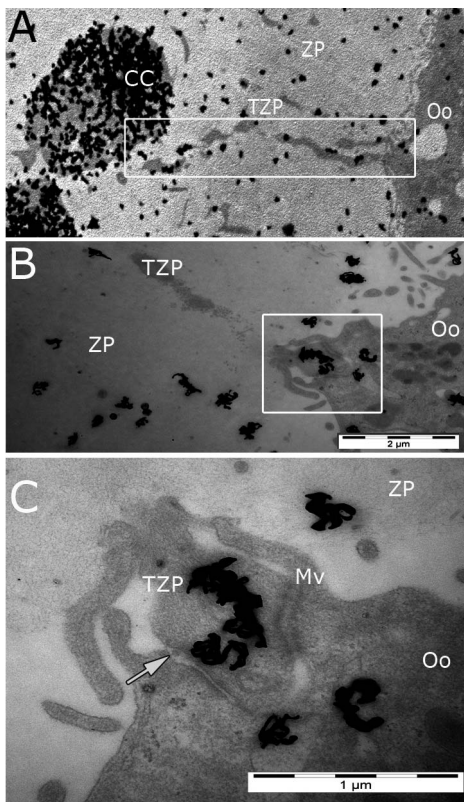


FIG. 1. Nascent RNA in the projections moves to the ooplasm. **A**) Autoradiographic signal from a 3-h exposure showing nascent RNA localization accumulating in the CC and directed down the TZPs through the zona pellucida (ZP) into the oocyte (Oo). **B**) Projection bulging end underneath the ZP and in contact with the oocyte. Strong RNA signal is present in the projection bulb and in the ooplasm opposed to the TZP. **C**) Magnified inset highlighted in **B**; microvilli (Mv) enveloping the TZP. The arrow indicates a vesicle.

and to recapitulate the natural difference in total RNA content found between the two states of maturation.

In the second RNA-seq experiment, sequencing of nascent RNA found in the TZPs was done using 110 COCs. Following oocyte collection, COCs were carefully hemisectioned using microdissection blades (Bioniche) so that the section containing the GV could be removed. This was confirmed with Hoechst 33342 (Life Technologies) labeling and brief epifluorescent imaging of DNA. Hemisectioned COCs were then matured in the presence of modified ethyl uridine (from the nascent RNA extraction kit; Life Technologies) for 9 h, a time coinciding with normal GV breakdown. Following this period of maturation, ZPs were then mechanically stripped of their cumulus cells and checked for contaminating cumulus cells using Hoechst staining. Total RNA was extracted from the isolated ZPs using the TRIzol method (Life Technologies), followed by isolation of the de novo RNA using the protocol accompanying the nascent RNA Capture Kit (Life Technologies). RNA-seq library preparation was conducted as described above. All sequencing reactions were carried out on a HiSeq2000 system (Illumina) for 200 cycles (services provided by Genome Québec Innovation Center, McGill University, Montréal, QC, Canada, and the Institut de Recherche en Immunologie et Cancérologie, Université de Montréal, Montréal, QC, Canada).

### Bioinformatics Analysis of RNA-seq Data

To remove read-through Illumina primers and the low-quality ends of sequences, all libraries were processed with the Cutadapt software. Cleaned sequences with a length smaller than 30 bp were then removed using Sickel (<https://github.com/ucdavis-bioinformatics/sickle/>). Only paired-end reads where both reads were longer than 30 nucleotides were kept. Average read length after cleanup and removal of read-through adaptors was 77 bp. Sequences were then aligned to the UMD3.1 assembly [23] of the bovine genome using TopHat2 software [24]. Alignments were quantified against a reference transcriptome using Cufflinks2 [25]. For the analysis of total RNA

from the GV and MII stages, normalization was conducted on the exogenous transcriptome (ERCC). Differential expression was assessed using *t*-tests. Further expression analysis of gene ontology and pathway enrichment was completed using DAVID [26, 27], using the cumulus cells' nascent transcriptome as background.

### Fixation and Fluorescent Staining

Labile direct stains were used to detect RNA and actin filaments. As often as possible, live oocytes were imaged as unfixed specimens to preserve their native structures. Actin staining was performed on oocytes fixed in 4% paraformaldehyde (Sigma-Aldrich) using rhodamine phalloidin (1:500 dilution; Cytoskeleton Inc.) and was used to specification. DNA was detected in oocytes after Hoechst 33342 staining (1:1000 dilution; Life Technologies). The SYTO RNaselect (1:1000 dilution; Life Technologies) was used for RNA staining on either live oocytes or those fixed with methanol, as was required for oocyte collection in the specific time periods after slaughter. After fixation and RNA staining, image analysis was conducted on maximum-intensity projections of equal thickness, 10 image slices per oocyte, taken at the largest diameter of each oocyte. The TZPs bearing RNA were then counted within each maximum-intensity projection. RNase treatments and untreated oocytes were imaged to ensure specificity of RNA labeling and a lack of confounding autofluorescence (Supplemental Fig. S1, Supplemental Data are available online at [www.biolreprod.org](http://www.biolreprod.org)). Fluorescent microscopy was carried out on a Zeiss LSM 740 confocal microscope using ZEN capture and image analysis software (Carl Zeiss Canada).

### Statistics

Oocytes were collected from abattoir ovaries, washed, and pooled together for morphological selection of quality gametes. Random sorting was carried out to create treated and control groups for all inhibitor work, RNAseq library construction, and functional assessments on rate of maturation in the presence of inhibitors. Comparison of means was carried out by either one-way ANOVA with Dunnett post hoc test when comparing treatments to controls only, by Bonferroni post hoc test when comparing multiple treatments, or by *t*-test comparing pairs of observations with significance attained at  $P < 0.05$ . Prism 5, Graphpad software was used for analysis.

## RESULTS

### RNA Localization and Movement in the COC

To demonstrate the localization of de novo RNA transcripts, [<sup>3</sup>H]-uridine was incorporated into maturing COCs. As shown in Figure 1, nascent RNA was detected within the TZPs of treated COCs. Abundant silver deposition was observed in the transcriptionally active nucleus of the cumulus cells, and also within other regions of their cytoplasm, including the TZP (Fig. 1A). A 3-h period of exposure to [<sup>3</sup>H]-uridine during early oocyte maturation resulted in the presence of labeling in the bulb of the projection (Fig. 1B). The signal exists in the tip of the TZP, and also across the membranous interaction in the ooplasm of the oocyte. Higher-magnification imaging was taken, and small vesicles were detected in the cleft between the two membranes (Fig. 1C).

Regional analysis of images for silver grain deposition as a percentage of total area (Fig. 2) demonstrated a significantly higher localization of signal in the cumulus cells ( $n = 10$  images of different oocytes), with a mean detection value of  $24.53\% \pm 3.1\%$  SEM; and in TZPs ( $n = 11$  images of different oocytes), with  $3.87\% \pm 0.71\%$  compared with the values obtained in the entire zona pellucida ( $n = 9$  images of different oocytes;  $0.42\% \pm 0.05\%$ ) and in the ooplasm ( $n = 9$ ;  $0.41\% \pm 0.06\%$ ). By comparison, the mean background found in “noncellular” regions of the images ( $n = 7$ ) was  $0.28\% \pm 0.06\%$ . All groups were significantly higher than control mean values from exposed slides without cellular material submitted to autoradiographic exposure (control BKG [ $n = 9$ ],  $0.09\% \pm 0.01\%$ ; Supplemental Fig. S2). These results support nascent RNA accumulation in the TZPs.

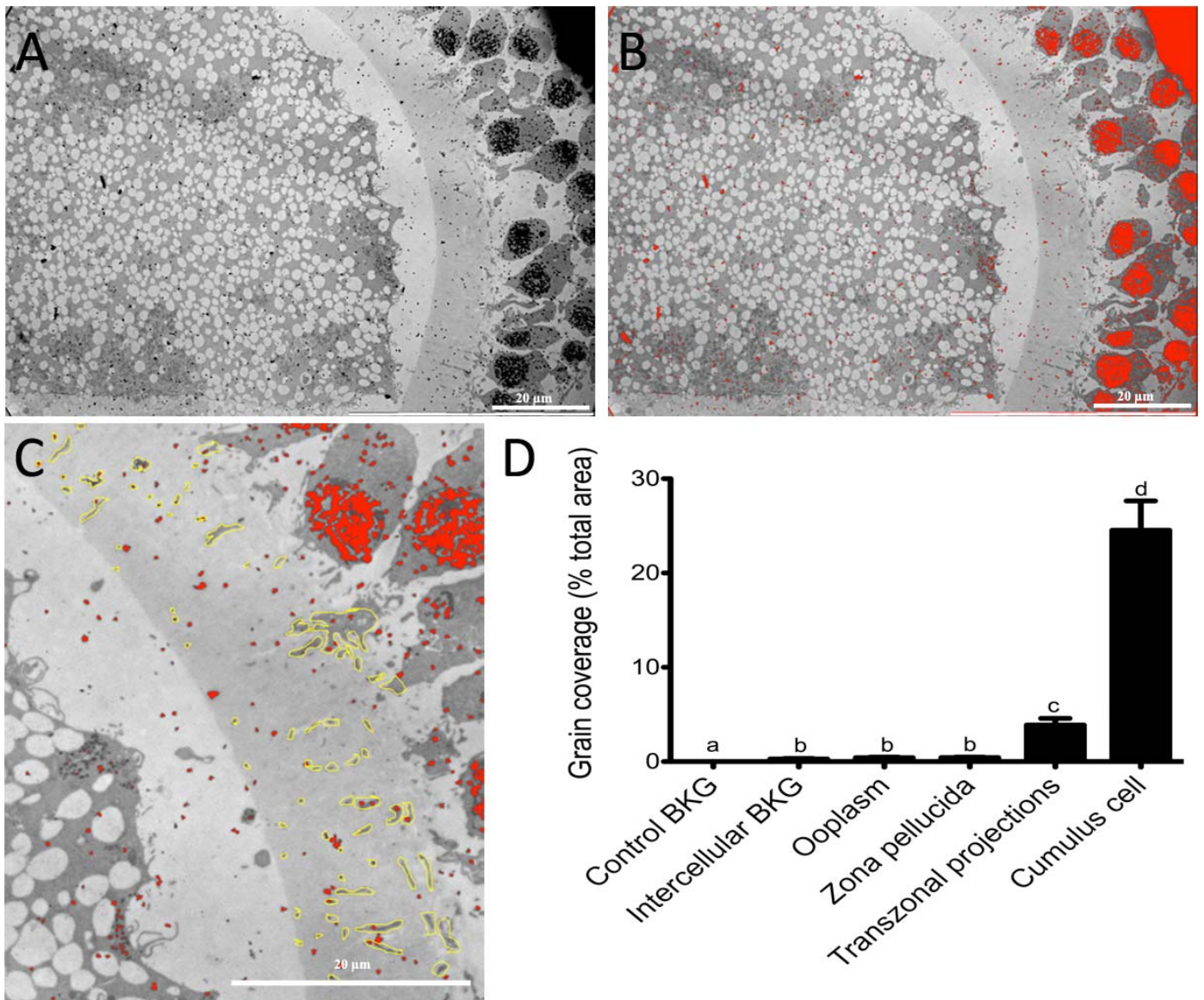


FIG. 2. Detection of nascent RNA within different regions of the COC. **A)** Original image of a semithin section after 3-h autoradiographic incorporation and exposure. **B)** Threshold detection of autoradiographic signal for analysis (red signal). **C)** RNA signal corresponding to the TZP's outlined in yellow within the zona pellucida (ZP). **D)** Quantification of RNA-associated signal for each of the regions of interest. BKG, background. Statistical significance is indicated when letters differ between treatments ( $P < 0.05$ ).

Evidence of active transfer of RNA from the cumulus cells to the oocyte was found by comparing the signal distribution of labeled nascent RNA within a fully enclosed oocyte with the signal detected in a partially denuded oocyte (Fig. 3, A and B). Although signals were homogeneously distributed in the oocyte surrounded by cumulus cells, a clear gradient was detected in the partially denuded counterpart, where concentrated RNA signal was observed proximal to the cumulus-bearing portion of the oocyte, and the distal and denuded portion of the oocyte contained sparse signal (Fig. 3, A and B). Signal detection in the GV's of similar sections was negligible and did not radiate outward into the ooplasm. To confirm this gradient occurrence, a second approach was used by fluorescently labeling nascent transcription followed by detection in cumulus-enclosed and partially denuded oocytes. None of the cumulus-enclosed oocytes ( $n = 9$  oocytes) showed any trend in regional signal difference (Fig. 3C), whereas of the 11 partially denuded oocytes evaluated, 8 demonstrated a significantly higher RNA

signal in the regions of ooplasm proximal to the cumulus cells compared with their distal regions ( $P < 0.05$ ). When the gradient plane was rotated  $180^\circ$ , the differences in signal intensity were lost (Fig. 3D). From both methodological approaches, results show the presence of nascent RNA from the cumulus cells inside the ooplasm.

Additionally, to confirm and visualize RNA movement from the cumulus cell toward the oocyte, total RNA staining in living COCs was carried out using confocal live cell imaging and revealed the displacement of RNA granules in TZPs (Fig. 4). Although some granules remained stationary, others moved either very quickly (micrometers per minute) or very slowly (micrometers per hour) within the cumulus cells (Fig. 4). The speed and direction of the moving granules were not always constant: some stopped or even changed direction for a short distance. A number of the particles, both fast (Fig. 4A) and slow (Fig. 4B) moving, transferred down the TZP toward the oocyte. Quantification of granule trafficking was done by time-

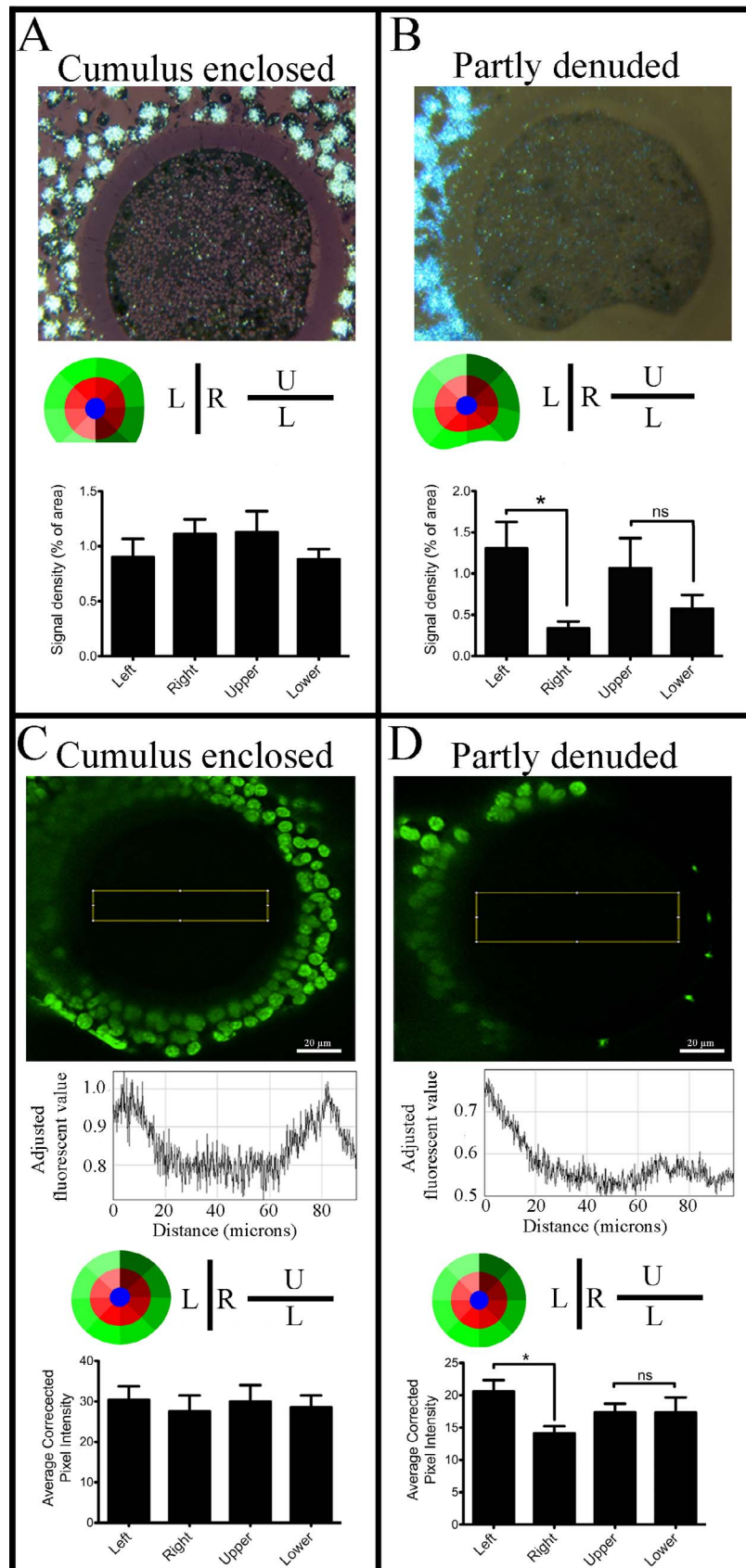


FIG. 3. Impact of the presence of cumulus cells on the presence of nascent RNA inside the oocyte. Comparison of nascent RNA detection levels between cumulus-enclosed oocytes and partly denuded ones. **A** and **B**) Quantification of autoradiographic signals from de novo RNA synthesis labeled by [<sup>3</sup>H]-uridine incorporation (magnification ×50). **C** and **D**) Nascent RNA was labeled by incorporation of 5-ethynyl-2'-deoxyuridine, to which a fluorescent dye was chemically bound (green signal). Pixel intensity was measured in regions (yellow boxes) proximal to distal from the cumulus cells in the ooplasm. Average regional signal intensity was corrected to actin detected by rhodamine phalloidin. For all analyses, the ooplasm was divided into left, right, upper, and lower planes based on the fitted pinwheel. Statistical significance was attained at  $P < 0.05$  (\*). ns, not significant.

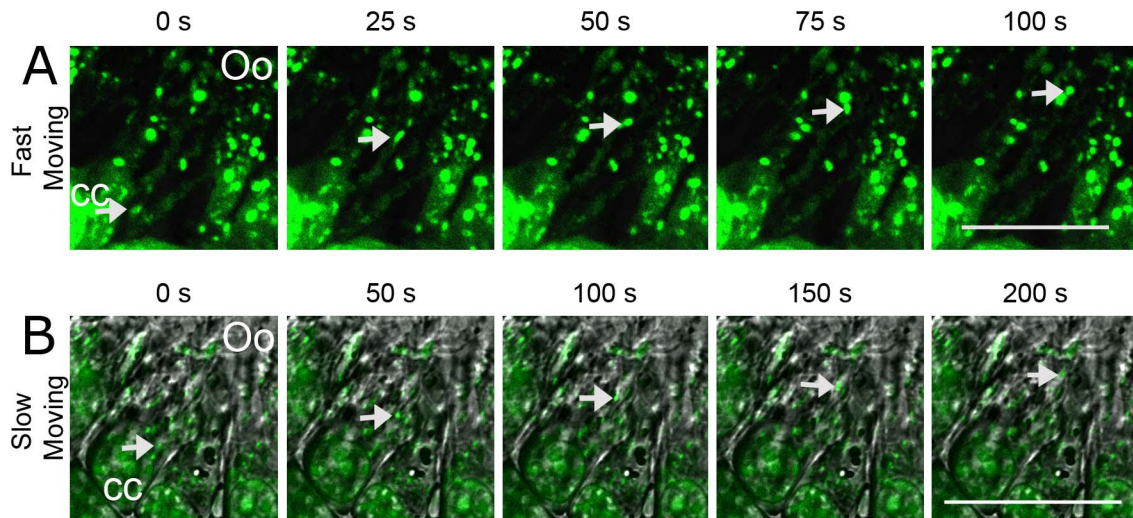


FIG. 4. Time series of moving granules in the cumulus cell projections toward the oocyte. **A)** Fast-moving granules present in sections taken 20 sec apart from each other. **B)** Slow-moving granules in frames taken 2 min apart from each other. Numerous other granules are present but move only slightly or remain stationary. The granules begin near the cumulus cell (CC) and move toward the oocyte (Oo) along the TZPs. Bars = 20  $\mu$ m. See also Supplemental Movies S1 and S2.

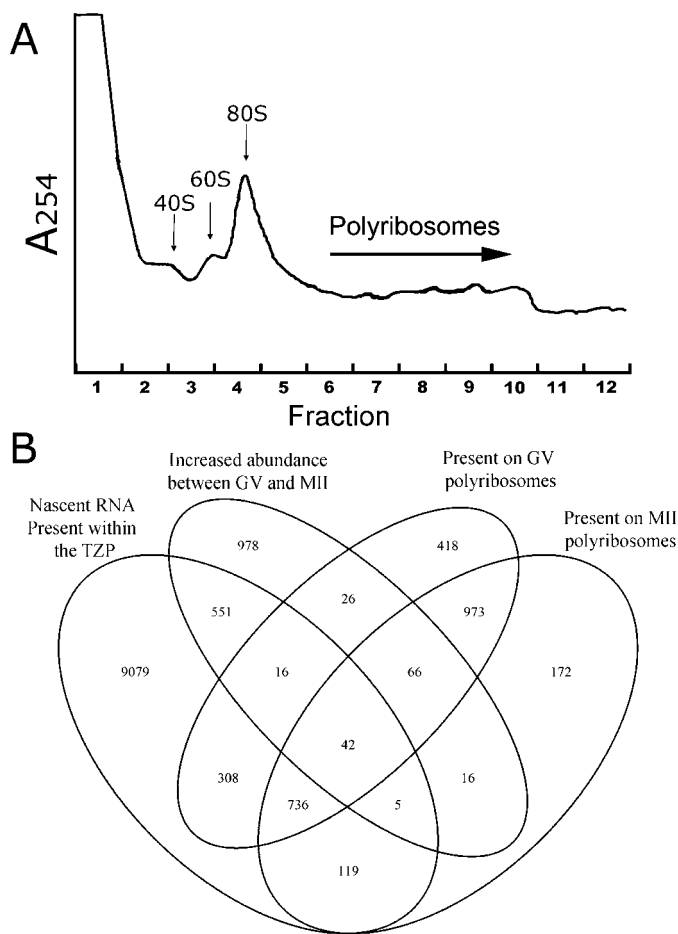


FIG. 5. Transcript identification in the different structural components of the COC. **A)** Sucrose density gradient profile outlining the fractionation of cellular extracts and position of polyribosomes. The profiles are generated from the spiked-in *Drosophila* polyribosomes used as a carrier, which allows identification of the proper fractions for confirmed polyribosomal RNAs. **B)** Venn diagram of identified bovine transcripts found in the TZP, increasing in abundance during the period of maturation, and present on the polyribosomes both in GV and MII oocytes.

lapse imaging of a static region near the zona pellucida. From  $7.0 \pm 1.0$ -min video recordings ( $n = 14$ ), each enabling the monitoring of an average of  $41.6 \pm 3.3$  projections,  $12.1 \pm 1.9$  granules were found to move toward the oocyte, whereas  $6.8 \pm 1.0$  granules displayed a retrograde progression. This occurrence and distribution of RNA granules within the TZPs is consistent with the results of the autoradiographic evaluation showing the extent of RNA granule distribution from the de novo RNA synthesis. Videos of RNA granule movement can be found in the supplemental data (Supplemental Movies S1 and S2).

#### *RNA Transcripts Present in the TZP Are Also Found on the Oocyte's Translational Machinery*

By identifying the transcripts synthesized by the cumulus cells during the first 9 h after extraction from the follicular environment, we recently reported that as much as 45% of the nascent transcripts found in the TZPs are specifically more abundant to this region of the cumulus cells compared with the nascent RNA population found in the cumulus cell body [19]. This selective distribution of long RNA molecules in the TZPs suggests potential roles for these transcripts in supporting cumulus-oocyte interactions as well as oocyte functions once transferred to the gamete. The transcriptomes of three subcompartments were analyzed, namely the newly synthesized transcripts found in TZPs, the oocyte contents at GV and MII stages, and the transcripts associated with the polyribosomes within the oocytes at the same developmental stages. The polyribosomal mRNAs represent the subfraction actively being translated to proteins (Fig. 5A). To evaluate the global potential for the TZP transcripts to be used by the oocyte, an analysis was done to generate a list of transcripts increasing in abundance within the oocyte during maturation. These transcripts found to be accumulating during maturation have potentially an exogenous origin, considering the cessation of oocyte transcription due to chromatin condensation [28].

Comparing this list to those found associated with the polyribosomes, 1226 transcripts intersected (Fig. 5B). From the transcripts identified, 624 were known mRNAs or long noncoding RNAs, whereas the remaining transcripts corresponded to uncharacterized transcripts (Supplemental Table

TABLE 1. Gene ontology terms enrichment for biological processes for transcripts found on the TZPs and the polyribosomes of GV and MII oocytes.

GO identification	Biological process	Count	%	P value
GO:0045449	Regulation of transcription	29	10.1399	0.0497
GO:0006355	Regulation of transcription, DNA-dependent	24	8.3916	0.0217
GO:0051252	Regulation of RNA metabolic process	24	8.3916	0.0261
GO:0008104	Protein localization	19	6.6434	0.0008
GO:0015031	Protein transport	17	5.9441	0.0018
GO:0045184	Establishment of protein localization	17	5.9441	0.0019
GO:0006396	RNA processing	13	4.5455	0.0024
GO:0046907	Intracellular transport	12	4.1958	0.0104
GO:0006412	Translation	11	3.8462	0.0270
GO:0007049	Cell cycle	10	3.4965	0.0399
GO:0007010	Cytoskeleton organization	9	3.1469	0.0090
GO:0022403	Cell cycle phase	8	2.7972	0.0110
GO:0043009	Chordate embryonic development	8	2.7972	0.0237
GO:0009792	Embryonic development ending in birth or egg hatching	8	2.7972	0.0244
GO:0032268	Regulation of cellular protein metabolic process	8	2.7972	0.0259
GO:0010629	Negative regulation of gene expression	8	2.7972	0.0298

S1). Gene list analysis showed enrichment for biological processes, such as transcript regulation, protein localization, protein transport, and RNA processing (Table 1), and molecular functions, such as nucleoside binding, ATP binding, RNA binding, and transcription factor binding (Table 2). A second, more stringent analysis was done, limiting the first list to include only transcripts from the ones identified in the TZPs following a pulse labeling of de novo transcription representing transcripts synthesized in the cumulus cells and sent to the TZPs. The gene list was reduced to 63 transcripts that were analyzed and showed enrichment for actin- and cytoskeleton-related biological processes: GO:0030036 actin cytoskeleton organization ( $P = 0.0024$ ); GO:0030029 actin filament-based process ( $P = 0.0026$ ); and GO:0007010 cytoskeleton organization ( $P = 0.0093$ ). These gene list analyses support a potential contribution from the cumulus cells in supplying the gamete with mRNAs coding for proteins involved in maturation-related processes.

*Timing of Developmental Competence Acquisition in Relation to RNA Accumulation in the TZPs*

The optimal intrafollicular preparation or prematuration time following animal slaughter for the acquisition of developmental competence was previously shown to be 4 h after slaughter [29]. This model of developmental competence acquisition was used to further study the potential role that TZP RNAs could play in oocyte quality and explore the temporal interaction between the oocyte and cumulus cells. Cumulus-oocyte complexes were collected from the ovarian follicles and

prepared for maturation either immediately or 4 h following slaughter (prematured groups). In addition, GV-stage oocytes were also stripped from their cumulus cells to determine the impact of the presence of the somatic cells on the rate of maturation (Fig. 6). As expected, the best maturation rate was obtained from the control treatment comprising intact COCs submitted to the 4-h postmortem incubation ( $79.5\% \pm 2.6\%$ ). This rate is not significantly different from our standard maturation system used in the previous experiments ( $78.4\% \pm 1.7\%$ ). Without the intrafollicular prematuration period, the rate of maturation of intact COCs significantly dropped ( $49.3\% \pm 4.0\%$ ). Comparable results were found when the COCs were allowed to pre-mature in vivo, followed by removal of the cumulus cells before IVM ( $52.3\% \pm 3.1\%$ ). The lowest maturation rates were obtained from oocytes collected without the pre-maturation period and immediately denuded and submitted to IVM ( $35.4\% \pm 4.6\%$ ).

Considering these results, where the impact of the cumulus cells on the oocyte was partly mitigated by their removal following the pre-maturation period, detection of total RNA in the TZPs was conducted following a time series starting at the time of slaughter and lasting until 6 h after slaughter (Fig. 7). Oocytes demonstrated an increasing number of RNA-bearing TZPs over time, significantly increasing between 0 h ( $35.8\% \pm 3.0\%$ ;  $n = 22$ ), 2 h ( $44.4\% \pm 3.5\%$ ;  $n = 25$ ), and 4 h ( $78.0\% \pm 4.4\%$ ;  $n = 26$ ) after slaughter, and appearing to plateau by 6 h ( $91.6\% \pm 4.9\%$ ;  $n = 28$ ; Fig. 7, A and B). The number of TZPs did not change over time as determined by actin staining from 0 h ( $165.1\% \pm 14.4\%$ ;  $n = 14$ ), to 2 h ( $201.7\% \pm 33.4\%$ ;  $n = 6$ ), to 4 h ( $213.6\% \pm 18.2\%$ ;  $n = 14$ ), and to 6 h ( $192.6\% \pm$

TABLE 2. Gene ontology terms enrichment for molecular functions for transcripts found in the TZPs and polyribosomes of MII and GV oocytes.

GO identification	Molecular function	Count	%	P value
GO:0001882	Nucleoside binding	30	10.4895	0.0241
GO:0005524	ATP binding	29	10.1399	0.0162
GO:0032559	Adenyl ribonucleotide binding	29	10.1399	0.0180
GO:0030554	Adenyl nucleotide binding	29	10.1399	0.0335
GO:0001883	Purine nucleoside binding	29	10.1399	0.0371
GO:0003723	RNA binding	13	4.5455	0.0228
GO:0008134	Transcription factor binding	11	3.8462	0.0001
GO:0008092	Cytoskeletal protein binding	9	3.1469	0.0461
GO:0004386	Helicase activity	7	2.4476	0.0072
GO:0019904	Protein domain-specific binding	6	2.0979	0.0340
GO:0008022	Protein C-terminus binding	5	1.7483	0.0058
GO:0008135	Translation factor activity, nucleic acid binding	5	1.7483	0.0365
GO:0003712	Transcription cofactor activity	5	1.7483	0.0472

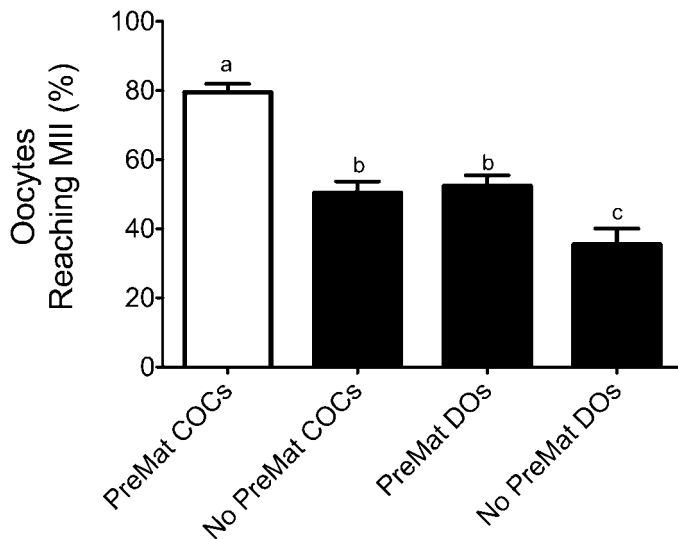


FIG. 6. Impact of time of intrafollicular prematuration and of somatic cell removal on oocyte maturation competence. Cumulus-oocyte complexes were aspirated from the follicular environment either immediately after slaughter (No PreMat) or following a 4-h postmortem incubation of the ovaries before COC collection (PreMat). The requirement of the presence of the cumulus cells for the beneficial effect from the prematuration incubation was tested by denuding the oocytes (DOs). Maturation rates were collected following in vitro culture of COCs and DOs. Statistical significance is indicated when letters differ between treatments ( $P < 0.05$ ).

13.1%;  $n = 14$ ; Fig. 7). This shows a postslaughter accumulation of transcripts in the TZPs under a timetable fitting with the positive effect of the prematuration period.

## DISCUSSION

The presented results highlight the additional contribution of the cumulus cells to the oocyte in the form of large cargo transfer. We focused on RNA transfer from the cumulus cells and its importance for gamete maturation. The current understanding of folliculogenesis and oogenesis involves a close interdependence between the cumulus cells and the oocyte, mediated through the extensive intercommunication that exists between these two compartments. The oocyte contributes to cumulus cell function via paracrine signaling with secreted proteins like GDF9 and BMP15 [14], while the cumulus cells transfer small molecules like the cyclic nucleotides cGMP and cAMP [30, 31], and energy sources like lactate, pyruvate, and phosphocreatine to the oocyte [32, 33]. We previously demonstrated that a synthetic transcript expressed in the cumulus cells could be transferred to the oocyte. The presence of the GFP fusion protein in the oocyte cytoplasm indicated translational activity, but it was not possible to determine whether the fusion protein was translated in the cumulus cell and then transferred, or translated in the oocyte [20]. This type of large cargo transfer is not well documented in mammalian oocytes but is present under different forms in other animal models, like *Caenorhabditis elegans* and *Drosophila*, where there are stages of material sharing during oocyte development, either from canals bridging oocytes together or from supporting nurse cells [34, 35].

The data from nascent autoradiographic RNA labeling show abundant RNA signal inside the oocyte, and that the presence of cumulus cells influenced signal distribution. These results were confirmed by fluorescent labeling of de novo transcription. The rate at which transfers occur is still undetermined.

However, because of the great number—likely more than 3000 actin-based TZPs per COC by our estimates—a large effect can be created on the oocyte's internal content even if particle transfer per TZP is not frequently abundant. From the ultrathin sections it was shown that some vesicles present at the junction of the projection end and the oolemma are not labeled, which is indicative that some of these secreted bodies either harbor non-RNA material or RNA that was produced prior to the labeling pulse. It is also noteworthy to mention that when detecting autoradiographic signal, the exact position and particle size may be shifted (in the order of a few nanometers) because of radiation and emulsion thickness. The large grain size can also possibly obscure the cellular structure in the section beneath the grain. Together, the data support directional transfer of RNA to the oocyte. The live-cell imaging confirmed that many RNA-containing granules remain stationary, whereas others move down the projections. The speed and direction (both anterograde and retrograde) of the particles that were tracked are not constant, an observation similar to findings observed in neurons where RNA particles move down the axon to be translated in the synapse [36].

Identification of these transcripts, potentially transferred from the cumulus cells to the oocyte in support of the maturation processes, was done by surveying the transcriptome of different compartments of the COCs. At this stage, the oocyte is already rich in maternal RNA reserves, making it uncertain that transferred transcripts would significantly add to the oocyte endowment. Maternal reserves are known to be stored under a stabilized form of ribonucleoprotein particles [37, 38]. Transcripts from the cumulus cells could be more readily available for translation than stored ones that require dissociation of the protein complex and readenylation of their poly(A) tails. We focused on a subset of transcripts shown to be common between the messengers enriched in the TZPs and those found on the oocyte's translational machinery. The function of the candidate mRNA fits with the known cellular functions associated with the control of meiosis resumption, namely nucleotide management, and transcriptional and translation control. In addition, several zinc finger mRNAs were found (ZNF773, ZNF689, ZNF75A, ZNF664, and ZNF395), all of which are known to bind DNA and regulate transcription in somatic cells [39, 40]. These DNA-binding proteins could be important for interactions during chromatin remodeling during meiosis. A number of gene pathways found in our analysis are common to those previously identified in the surveys of the transcripts found during mouse oocyte maturation [41].

A more stringent sorting identified the subset of transcripts that are common to the TZPs and polyribosomes but also increased in abundance in the oocyte during maturation. This last criterion represents transcripts that are increasing in abundance when the oocyte's transcription is believed to be silenced [42, 43], thus providing good candidates to be originating from the cumulus cells. This limited gene list is associated with the organization of the cytoskeleton, particularly with the actin filaments and canonical beta-catenin signaling. It is known that actin filaments create polarity in the oocytes as the polar body is extruded [44], and that they are responsible for enabling the asymmetric cellular division [45]. Specifically, the FAM21 (family with sequence similarity 21, member C) and WASF2 (WAS protein family, member 2) transcripts were present in our list and are members of the WASH complex (Wiskott Aldrich Syndrome protein and scar homologue complex), which regulates the actin-regulating protein complexes (Arp1/2) [46]. Canonical beta-catenin signaling components like paxillin (PXN), which facilitates

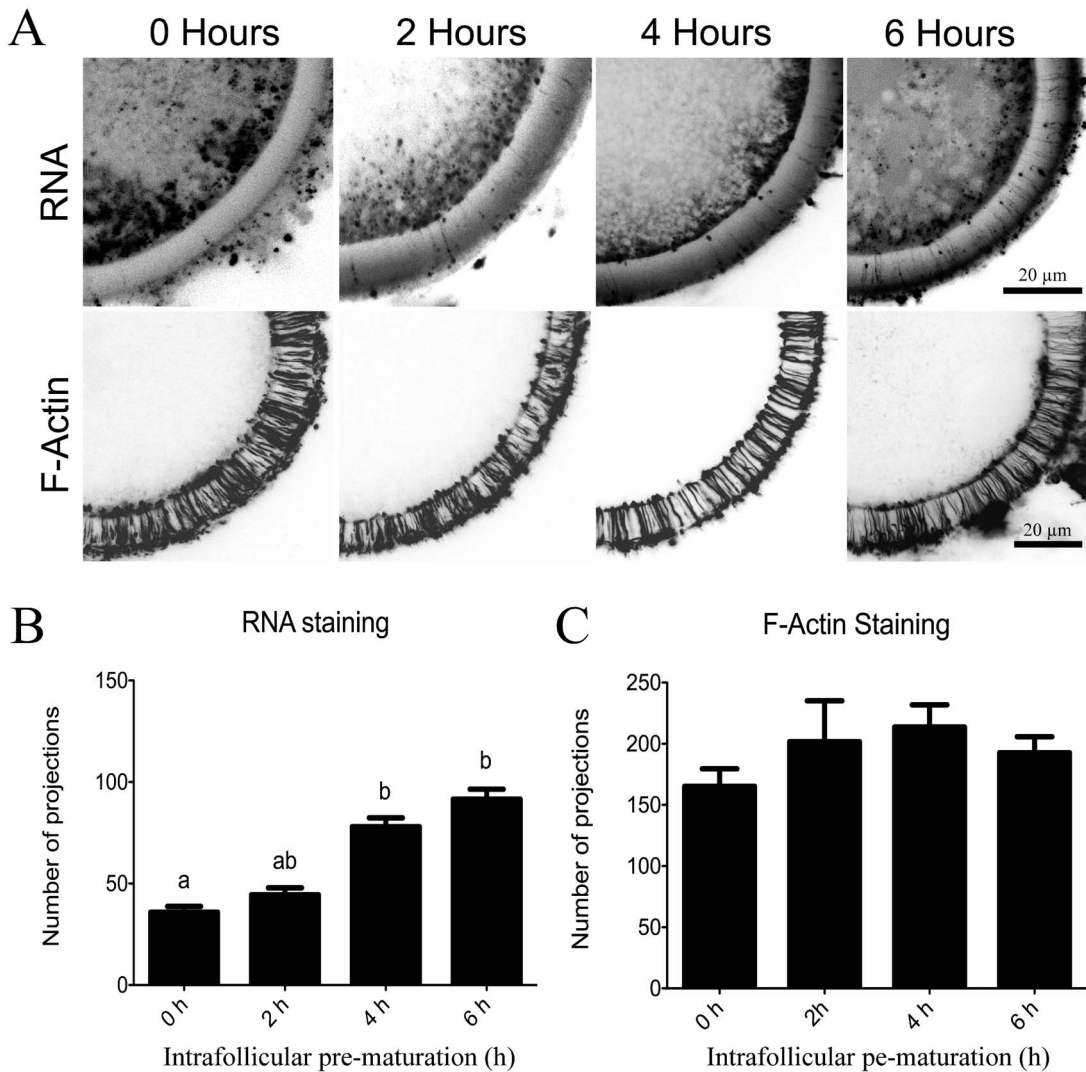


FIG. 7. Timing of TZPs' RNA loading. **A**) Maximum-intensity projections of the equatorial cross sections of the oocytes stained for RNA (SytoRNA select) and F-Actin (rhodamine phalloidin) after recovery from ovaries 0, 2, 4, and 6 h postmortem, the intrafollicular pre-maturation periods. **B**) Quantification of projections containing detectable RNA signals along the postmortem wait before oocyte recovery from the ovaries. **C**) Total number of actin-stained TZP structures at each time point. Statistical significance is indicated when letters differ between treatments ( $P < 0.05$ ).

actin-membrane attachment and behaves as a signal integrator [47, 48], and frizzled class receptor 3 (FZD3), a frizzled family member that encodes a seven-transmembrane domain protein that is involved in wntless-type MMTV integration site family member 2 (WNT2) signaling [49], were also present. These genes have been associated with oocyte quality in aging women [44]. A final transcript of interest is the transcriptional repressor spen family transcriptional repressor (SPEN, also known as SHARP). This mRNA codes for a hormone-inducible transcription repressor that contains RNA recognition motifs that confer steroid receptor RNA coactivation [50]. SPEN also allows for interaction with the nucleosome remodeling deacetylase complex (NuRD complex), which may confer epigenetic regulation to the oocyte [51]. At this time, further study is needed to provide the full proof specific to each of these mRNAs that are produced by the somatic cells and transferred to the oocyte. Our results do provide a body of evidence that supports the transfer of these candidates.

If these transcripts are supporting maturation and oocyte quality, given that TZPs are established early during folliculogenesis, the next question to be asked is if the RNA content in these structures stays constant or fluctuates during folliculo-

genesis. The initial survey done during the *in vitro* incubation period, starting after aspiration from the ovarian follicles up to the disconnection that occurs during maturation, did not show evidence of total RNA content fluctuation [20]. However, it is believed that at the time of aspiration, oocyte quality expressed as developmental competence is already established from unknown cues occurring earlier inside the follicle. As a model of oocyte quality, we used observations from a previous study showing that oocytes collected from medium-size antral follicles from ovaries collected postmortem displayed a progressive acquisition of developmental competence according to the duration before the oocytes were extracted from the follicles [12]. It was noticed that oocytes collected immediately postmortem display poor developmental competence, whereas a 4-h postmortem incubation of the ovaries maximized developmental rates [12]. At this point it was not known whether the reduced developmental capacity of a COC removed from the follicle immediately after animal death was caused by an impairment to complete maturation or by impairment to sustaining early development. We confirmed that the oocyte's capacity to reach MII is affected by the timing of intrafollicular incubation prior to COC retrieval. Collecting

the COCs immediately significantly reduced the potential to mature. Using this system we show that TZPs contain little RNA before the onset of the unknown initiating events, following which the gamete improves its ability to mature. RNA accumulates in the TZPs following a timetable similar to that of the acquisition of developmental competence, which has been previously published [29].

The nature of the mechanisms underlying this positive effect on oocyte quality is still unknown. Several conditions have been shown to increase developmental competence: the luteinizing hormone surge, the timing before oocyte aspiration following animal death [12], and the removal of the growth support [9, 10]. Luteinizing hormone triggers disconnection between the follicular cells that will induce differentiation and corpus luteum formation [52]. Animal death or loss of hormonal support can also initiate the disconnection associated with follicle demise [9, 10]. Signaling pathways common to these events could explain why stressors induce competence in the oocyte. In the present study, we called “prematuration” this period where the oocyte benefits from these unknown cues within the follicle to increase its developmental competence, still under meiotic arrest. The TZP RNA loading not only fit well with the timing of the acquisition of developmental competence as described in this situation of postmortem incubation before oocyte aspiration, it was also shown that preventing the RNA accumulation by maturing the COCs in vitro immediately after slaughter significantly reduced their capacity to reach MII. The cumulus contribution is known to be important, and denuded oocytes mature at rates much lower than those of their enclosed counterparts, and coculturing COCs with denuded oocytes can recover some of the potential lost with denudation [33, 53, 54]. In this study, the worst-case scenario was achieved when oocytes were immediately collected from the follicle postmortem and stripped of their cumulus cells to remove the contribution from the cumulus cells. Based on the results, this quick removal from the follicular environment prevented TZP loading, and stripping the cumulus cells removed any potential to do so, even for a short period during the onset of maturation in vitro. Removing both of these opportunities for cumulus cell contribution reduced the oocyte’s potential to mature.

In conclusion, we propose a new contribution from the cumulus cells to the oocyte that is integral to maturation. We show that TZP loading with RNA mainly occurs within the follicles prior to oocyte extraction; thus, a physiological event is responsible for the mobilization of RNA. This transfer of RNA to the oocyte complements the maturation control mediated by cAMP signaling in the COC. This opens new avenues to the concept of oocyte quality as the mechanisms initiating and controlling TZP transcript accumulation remain to be described. Yet at this point, we can only associate the contribution of the cumulus cells to the oocyte’s capacity to mature. Any contribution to embryo development remains to be further investigated. This new concept offers novel perspectives about female fertility and for IVM improvement.

## ACKNOWLEDGMENT

We thank L. St. John, I. Dufort, I. Laflamme, and H. Holm for their technical assistance during this project. We thank Dr. Allan King for providing laboratory space to complete the data on inhibitors. We also thank Boviteq Inc. for its support for providing the medium and portable incubator for off-site oocyte maturation.

## REFERENCES

1. Edwards RG. Maturation in vitro of mouse, sheep, cow, pig, rhesus monkey and human ovarian oocytes. *Nature* 1965; 208:349–351.
2. Trounson A, Anderiesz C, Jones G. Maturation of human oocytes in vitro and their developmental competence. *Reproduction* 2001; 121:51–75.
3. Rizos D, Ward F, Duffy P, Boland MP, Lonergan P. Consequences of bovine oocyte maturation, fertilization or early embryo development in vitro versus in vivo: implications for blastocyst yield and blastocyst quality. *Mol Reprod Dev* 2002; 61:234–248.
4. Guzman LM, Ortega-Hrepich C, Albuz F, Verheyen G, Devroey P, Smits J, De Vos M. Developmental capacity of in vitro-matured human oocytes retrieved from polycystic ovary syndrome ovaries containing no follicles larger than 6 mm. *Fertil Steril* 2012; 98:503–507.e2.
5. Walls ML, Hunter T, Ryan JP, Keelan JA, Nathan E, Hart RJ. In vitro maturation as an alternative to standard in vitro fertilization for patients diagnosed with polycystic ovaries: a comparative analysis of fresh, frozen and cumulative cycle outcomes. *Hum Reprod* 2014; 30:88–96.
6. Rizos D. Bovine embryo culture in the presence or absence of serum: implications for blastocyst development, cryotolerance, and messenger RNA expression. *Biol Reprod* 2002; 68:236–243.
7. Albuz FK, Sasseville M, Lane M, Armstrong DT, Thompson JG, Gilchrist RB. Simulated physiological oocyte maturation (SPOM): a novel in vitro maturation system that substantially improves embryo yield and pregnancy outcomes. *Hum Reprod* 2010; 25:2999–3011.
8. Gad A, Hoelker M, Besenfelder U. Molecular mechanisms and pathways involved in bovine embryonic genome activation and their regulation by alternative in vivo and in vitro culture conditions. *Biol Reprod* 2012; 87: 100.
9. Blondin P, Bousquet D, Twagiramungu H, Barnes F, Sirard MA. Manipulation of follicular development to produce developmentally competent bovine oocytes. *Biol Reprod* 2002; 66:38–43.
10. Nivet AL, Bunel A, Labrecque R, Belanger J, Vigneault C, Blondin P, Sirard MA. FSH withdrawal improves developmental competence of oocytes in the bovine model. *Reproduction* 2012; 143:165–171.
11. Plourde D, Vigneault C, Lemay A, Breton L, Gagné D, Laflamme I, Blondin P, Robert C. Contribution of oocyte source and culture conditions to phenotypic and transcriptomic variation in commercially produced bovine blastocysts. *Theriogenology* 2012; 78:116–131.e3.
12. Blondin P, Sirard MA. Oocyte and follicular morphology as determining characteristics for developmental competence in bovine oocytes. *Mol Reprod Dev* 1995; 41:54–62.
13. Le Beux G, Richard FJ, Sirard MA. Effect of cycloheximide, 6-DMAP, roscovitine and butyrolactone I on resumption of meiosis in porcine oocytes. *Theriogenology* 2003; 60:1049–1058.
14. Hussein TS, Thompson JG, Gilchrist RB. Oocyte-secreted factors enhance oocyte developmental competence. *Dev Biol* 2006; 296:514–521.
15. Yeo CX, Gilchrist RB, Lane M. Disruption of bidirectional oocyte-cumulus paracrine signaling during in vitro maturation reduces subsequent mouse oocyte developmental competence. *Biol Reprod* 2009; 80: 1072–1080.
16. Gilchrist RB, Lane M, Thompson JG. Oocyte-secreted factors: regulators of cumulus cell function and oocyte quality. *Hum Reprod Update* 2008; 14:159–177.
17. Hyttel P, Fair T, Callesen H, Greve T. Oocyte growth, capacitation and final maturation in cattle. *Theriogenology* 1997; 47:23–32.
18. Albertini DF, Barrett SL. The developmental origins of mammalian oocyte polarity. *Semin Cell Dev Biol* 2004; 15:599–606.
19. Moor RM, Smith MW, Dawson RM. Measurement of intercellular coupling between oocytes and cumulus cells using intracellular markers. *Exp Cell Res* 1980; 126:15–29.
20. Macaulay AD, Gilbert I, Caballero J, Barreto R, Fournier E, Tossou P, Sirard MA, Clarke HJ, Khandjian EW, Richard FJ, Hyttel P, Robert C. The gametic synapse: RNA transfer to the bovine oocyte. *Biol Reprod* 2014; 91:90.
21. Faerge I, Grondahl C, Ottesen JL, Hyttel P. Autoradiographic localization of specific binding of meiosis-activating sterol to cumulus-oocyte complexes from marmoset, cow, and mouse. *Biol Reprod* 2001; 64: 527–536.
22. Scantland S, Grenon JP, Desrochers MH, Sirard MA, Khandjian EW, Robert C. Method to isolate polyribosomal mRNA from scarce samples such as mammalian oocytes and early embryos. *BMC Dev Biol* 2011; 11: 8.
23. Robert C, Nieminen J, Dufort I, Gagné D, Grant JR, Cagnone G, Plourde D, Nivet AL, Fournier E, Paquet É, Blazejczyk M, Rigault P, et al. Combining resources to obtain a comprehensive survey of the bovine

- embryo transcriptome through deep sequencing and microarrays. *Mol Reprod Dev* 2011; 78:651–664.
24. Zimin AV, Delcher AL, Florea L, Kelley DR, Schatz MC, Puiu D, Hanrahan F, Pertea G, Van Tassell CP, Sonstegard TS, Marçais G, Roberts M, et al. A whole-genome assembly of the domestic cow, *Bos taurus*. *Genome Biol* 2009; 10:R42.
  25. Kim D, Pertea G, Trapnell C, Pimentel H, Kelley R, Salzberg SL. TopHat2: accurate alignment of transcriptomes in the presence of insertions, deletions and gene fusions. *Genome Biol* 2013; 14:R36.
  26. Roberts A, Pimentel H, Trapnell C, Pachter L. Identification of novel transcripts in annotated genomes using RNA-Seq. *Bioinformatics* 2011; 27:2325–2329.
  27. Huang DW, Sherman BT, Lempicki RA. Bioinformatics enrichment tools: paths toward the comprehensive functional analysis of large gene lists. *Nucleic Acids Res* 2009; 37:1–13.
  28. Huang DW, Sherman BT, Lempicki RA. Systematic and integrative analysis of large gene lists using DAVID bioinformatics resources. *Nat Protoc* 2008; 4:44–57.
  29. Blondin P, Guilbault LA, Sirard MA. In vitro production of bovine embryos: developmental competence is acquired before maturation. *Theriogenology* 1995; 43:168.
  30. Richard FJ, Fortier MA, Sirard MA. Role of the cyclic adenosine monophosphate-dependent protein kinase in the control of meiotic resumption in bovine oocytes cultured with thecal cell monolayers. *Biol Reprod* 1997; 56:1363–1369.
  31. Wigglesworth K, Lee KB, O'Brien MJ, Peng J, Matzuk MM, Eppig JJ. Bidirectional communication between oocytes and ovarian follicular somatic cells is required for meiotic arrest of mammalian oocytes. *Proc Natl Acad Sci U S A* 2013; 110:E3723–E3729.
  32. Scantland S, Tessaro I, Macabelli CH, Macaulay AD, Cagnone G, Fournier E, Luciano AM, Robert C. The adenosine salvage pathway as an alternative to mitochondrial production of ATP in maturing mammalian oocytes. *Biol Reprod* 2014; 91:75–75.
  33. Sutton-McDowall ML, Gilchrist RB, Thompson JG. The pivotal role of glucose metabolism in determining oocyte developmental competence. *Reproduction* 2010; 139:685–695.
  34. Wolke U, Jezuit EA, Priess JR. Actin-dependent cytoplasmic streaming in *C. elegans* oogenesis. *Development* 2007; 134:2227–2236.
  35. Nicolas E, Chenouard N, Olivo-Marin JC, Guichet AA. Dual role for actin and microtubule cytoskeleton in the transport of Golgi units from the nurse cells to the oocyte across ring canals. *Mol Biol Cell* 2009; 20:556–568.
  36. Davidovic L, Jaglin XH, Lepagnol-Bestel AM, Tremblay S, Simonneau M, Bardoni B, Khandjian EW. The fragile X mental retardation protein is a molecular adaptor between the neurospecific KIF3C kinesin and dendritic RNA granules. *Hum Mol Genet* 2007; 16:3047–3058.
  37. Flemr M, Ma J, Schultz RM, Svoboda P. P-body loss is concomitant with formation of a messenger RNA storage domain in mouse oocytes. *Biol Reprod* 2010; 82:1008–1017.
  38. Swetloff A, Conne B, Huarte J, Pitetti JL, Nef S, Vassalli JD. Dcp1-bodies in mouse oocytes. *Mol Biol Cell* 2009; 20:4951–4961.
  39. Laity JH, Lee BM, Wright PE. Zinc finger proteins: new insights into structural and functional diversity. *Curr Opin Struct Biol* 2001; 11:39–46.
  40. Burdach J, O'Connell MR, Mackay JP, Crossley M. Two-timing zinc finger transcription factors liaising with RNA. *Trends Biochem Sci* 2012; 37:199–205.
  41. Su YQ, Sugiura K, Woo Y, Wigglesworth K, Kamdar S, Affourtit J, Eppig JJ. Selective degradation of transcripts during meiotic maturation of mouse oocytes. *Dev Biol* 2007; 302:104–117.
  42. Lodde V, Modina S, Maddox-Hyttel P, Franciosi F, Lauria A, Luciano AM. Oocyte morphology and transcriptional silencing in relation to chromatin remodeling during the final phases of bovine oocyte growth. *Mol Reprod Dev* 2008; 75:915–924.
  43. Fair T, Hulshof S, Hyttel P, Greve T. Nucleus ultrastructure and transcriptional activity of bovine oocytes in preantral and early antral follicles. *Mol Reprod Dev* 1997; 46:208–215.
  44. Cotichio G, Guglielmo MC, Albertini DF, Dal Canto M, Mignini Renzini M, De Ponti E, Fadini R. Contributions of the actin cytoskeleton to the emergence of polarity during maturation in human oocytes. *Mol Hum Reprod* 2014; 20:200–207.
  45. Yi K, Rubinstein B, Unruh JR, Guo F, Slaughter BD, Li R. Sequential actin-based pushing forces drive meiosis I chromosome migration and symmetry breaking in oocytes. *J Cell Biol* 2013; 200:567–576.
  46. Wang F, Zhang L, Zhang GL, Wang ZB, Cui XS, Kim NH, Sun SC. WASH complex regulates Arp2/3 complex for actin-based polar body extrusion in mouse oocytes. *Sci Rep* 2014; 4:5596.
  47. Sen A, Prizant H, Hammes SR. Understanding extranuclear (nongenomic) androgen signaling: what a frog oocyte can tell us about human biology. *Steroids* 2011; 76:822–828.
  48. Hammes SR, Levin ER. Minireview: recent advances in extranuclear steroid receptor actions. *Endocrinology* 2011; 152:4489–4495.
  49. Wang HX, Tekpetey FR, Kidder GM. Identification of WNT/ -CATENIN signaling pathway components in human cumulus cells. *Mol Hum Reprod* 2009; 15:11–17.
  50. Hatchell EC, Colley SM, Beveridge DJ, Epis MR, Stuart LM, Giles KM, Redfern AD, Miles LEC, Barker A, MacDonald LM, Arthur PG, Lui JCK, et al. SLIRP, a small SRA binding protein, is a nuclear receptor corepressor. *Mol Cell* 2006; 22:657–668.
  51. Ariyoshi M, Schwabe JWR. A conserved structural motif reveals the essential transcriptional repression function of Spen proteins and their role in developmental signaling. *Genes Dev* 2003; 17:1909–1920.
  52. Park JY. EGF-like growth factors as mediators of LH action in the ovulatory follicle. *Science* 2004; 303:682–684.
  53. Dey SR, Deb GK, Ha AN, Lee JI, Bang JI, Lee KL, Kong IK. Coculturing denuded oocytes during the in vitro maturation of bovine cumulus oocyte complexes exerts a synergistic effect on embryo development. *Theriogenology* 2012; 77:1064–1077.
  54. Luciano AM, Lodde V, Beretta MS, Colleoni S, Lauria A, Modina S. Developmental capability of denuded bovine oocyte in a co-culture system with intact cumulus-oocyte complexes: role of cumulus cells, cyclic adenosine 3',5'-monophosphate, and glutathione. *Mol Reprod Dev* 2005; 71:389–397.